JOURNAL OF COMPUTATIONAL PHYSICS 51, 65–82 (1983)

Constrained Finite Elements for Singular Boundary Value Problems

G. OGEN AND B. SCHIFF

School of Mathematical Sciences, Tel-Aviv University, Ramat-Aviv, Tel-Aviv, Israel

Received November 25, 1981; revised September 14, 1982

The finite element procedure for elliptic boundary value problems has been modified to deal with a boundary singularity. The mesh is refined locally, and the nodal values in the refinement region are constrained to agree with the known form of the solution in series, truncated after a finite number of terms. Solution of the finite element equations yields the coefficients in this series, together with the nodal values exterior to the refinement region, which constitutes a conforming super-element. The method has been applied to a model problem in two-dimensional fracture mechanics. The stress intensity factor is obtained directly and, together with the nodal displacements, is in good agreement with previous results.

1. INTRODUCTION

During the last decade various extensions have been made to the standard finite element procedure in order to enable it to deal with singular boundary value problems. The resulting techniques have been utilized extensively in fracture mechanics, in particular to compute stress intensity factors for various geometries.

Two basic approaches have been developed to allow for the presence of a singularity. In one approach, exemplified by [1–3], the usual elements are used, but the mesh is refined locally in the neighbourhood of the singularity. The other approach takes into account the known form of the solution near the singular point. In Refs. [4, 6–9], for example, singular functions are included explicitly in the trial function space, these functions being confined in most of the methods to a single element surrounding the tip of the re-entrant corner where the singularity occurs. In [5], on the other hand, special isoparametric elements are used, the singularity being introduced via the transformation.

The method of local mesh refinement has the disadvantage of considerably increasing the number of degrees of freedom, whilst the use of special elements makes the computational algorithm cumbersome.

In this work we try to combine these two approaches. We still use conventional elements and refine the mesh in the neighbourhood of the singularity, but on the other hand utilize the known asymptotic form of the singular solution in order to greatly reduce the number of degrees of freedom in the refined region.

0021-9991/83 $3.00

In Section 2 we explain the method and in Section 3 we apply it to a model problem and compare the results with those obtained by other methods.

2. A Modified Finite Element Approach

Let D be a two dimensional domain with a single re-entrant corner on its boundary (Fig. 1).

Let $\mathbf{u}(x, y)$ be the solution of a boundary value problem over D, expressed either in differential or in variational form. We assume that in the neighbourhood of the re-entrant corner, $\mathbf{u}(x, y)$ may be represented by the series

$$\sum_{i=1}^{\infty} a_i \mathbf{f}_i(x, y), \tag{1}$$

where $\mathbf{f}_i(x, y)$ are known functions.

We set up a mesh of rectangular elements in the following manner. We divide the entire domain D into three regions (Fig. 2.)

The interior region D_{in} consists of a rectangle surrounding the tip of the re-entrant corner. D_{out} denotes the exterior region up to the boundary ∂D, and D_{tr} is a transition strip between D_{in} and D_{out}.

In D_{out} we use the usual bilinear elements.

In D_{in} we still use bilinear trial functions in each rectangle, but the nodal values are no longer taken to be independent of one another. Instead, we require the values of $\mathbf{u}$ to satisfy the series (1), truncated after l terms, at each mesh point of D_{in}. Thus we have

$$\mathbf{q}_j = \sum_{m=1}^{l} a_m \mathbf{f}_m(x_j, y_j), \tag{2}$$

where $\mathbf{q}_j$ denotes the vector of the nodal values at the mesh point (x_j, y_j).

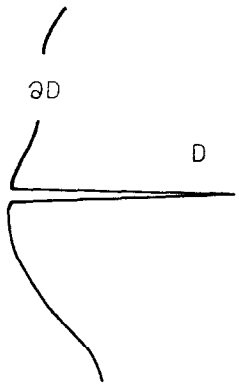

Fig. 1. Re-entrant corner on the boundary of D.

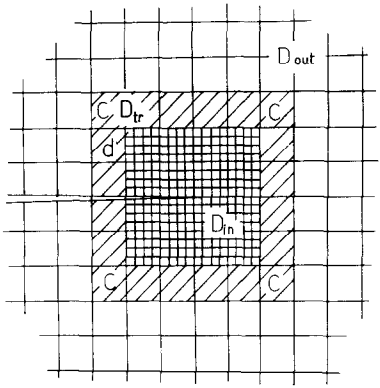

FIG. 2. Refinement region surrounding the singular point.

The unknowns in the region D_{in} will therefore be $a_1,\ldots,a_l$ instead of the nodal values, and we are in effect solving the variational problem subject to the constraints expressed by (2). The trial function over each element in D_{in} will thus be the bilinear interpolant to the values of the truncated series at the four corners.

We formulate the method in detail as follows. Let e be an element of D_{in}. Denote by $\mathbf{q}_e$ the vector of the nodal values in e, and by S_e the corresponding element stiffness matrix obtained for a bilinear trial function. In our model problem, we will use congruent rectangles of identical orientation, so evidently S_e will be the same for each element of D_{in}.

We can write $\mathbf{q}_e$ in the form

$$\mathbf{q}_e = A_e \mathbf{a}, \tag{3}$$

where $\mathbf{a}$ is the vector $(a_1,\ldots,a_l)^T$. The rows of the matrix A_e are grouped in four blocks, corresponding to the four corners, the number of rows in each block being equal to the dimension of the vector of the nodal values at one corner. For instance, if in each corner there are two nodal values, A_e will be as follows.

$$A_e = \begin{bmatrix} f_1^{(1)}(x_1,y_1) & f_2^{(1)}(x_1,y_1) & \cdots & f_l^{(1)}(x_1,y_1) \\ f_1^{(2)}(x_1,y_1) & f_2^{(2)}(x_1,y_1) & \cdots & f_l^{(2)}(x_1,y_1) \\ \vdots & \vdots & \vdots & \vdots \\ f_1^{(1)}(x_4,y_4) & f_2^{(1)}(x_4,y_4) & \cdots & f_l^{(1)}(x_4,y_4) \\ f_1^{(2)}(x_4,y_4) & f_2^{(2)}(x_4,y_4) & \cdots & f_l^{(2)}(x_4,y_4) \end{bmatrix} \tag{4}$$

In terms of the new variables the stiffmess matrix will be

$$S_e^* = A_e^T S_e A_e, \tag{5}$$

and this is the form used in the assembly.

Finally we consider the elements of D_{tr}. Let d in Fig. 3 be a typical element in D_{tr}, not one of the four corner elements denoted by c in Fig. 2.

Let $\mathbf{Q}_i$, $\mathbf{Q}_j$ be the vectors of the nodal values at the two mesh points common to d and the adjacent element in D_{out}. We divide the side of d adjacent to D_{in} into n equal parts, and this enables us to divide d into n equal rectangular elements as in Fig. 3. Let $\mathbf{q}_i^{(k)}$, $i = 1, 2, 3, 4$, be the nodal value vectors at the corners of the kth subelement d_k in d.

By taking

$$\mathbf{q}_3^{(k)} = \left(1 - \frac{k}{n}\right)\mathbf{Q}_i + \frac{k}{n}\mathbf{Q}_j,$$

$$\mathbf{q}_4^{(k)} = \left(1 - \frac{k-1}{n}\right)\mathbf{Q}_i + \frac{k-1}{n}\mathbf{Q}_j, \qquad k = 1, 2, \ldots, n, \tag{6}$$

the conforming condition is fulfilled between d_k and the neighbouring elements. Denoting by $\mathbf{q}^{(k)}$ the vector of all the nodal values in d_k and substituting $\mathbf{q}_1^{(k)}$ and $\mathbf{q}_2^{(k)}$ as in (2) we have

$$\mathbf{q}^{(k)} = A_k \mathbf{a}^*, \tag{7}$$

where $\mathbf{a}^*$ is a vector whose components are $a_1, \ldots, a_l$ and the components of $\mathbf{Q}_i$ and $\mathbf{Q}_j$. The matrix A_k, assuming again two nodal values at each corner, will be

$$\begin{bmatrix}
f_1^{(1)}(x_1, y_1) & \cdots & f_l^{(1)}(x_1, y_1) & 0 & 0 & 0 & 0 \\
f_1^{(2)}(x_1, y_1) & \cdots & f_l^{(2)}(x_1, y_1) & 0 & 0 & 0 & 0 \\
f_1^{(1)}(x_2, y_2) & \cdots & f_l^{(1)}(x_2, y_2) & 0 & 0 & 0 & 0 \\
f_1^{(2)}(x_2, y_2) & \cdots & f_l^{(2)}(x_2, y_2) & 0 & 0 & 0 & 0 \\
0 & 0 & 1 - \frac{k}{n} & 0 & \frac{k}{n} & 0 \\
0 & 0 & 0 & 1 - \frac{k}{n} & 0 & \frac{k}{n} \\
0 & 0 & 1 - \frac{k-1}{n} & 0 & \frac{k-1}{n} & 0 \\
0 & 0 & 0 & 1 - \frac{k-1}{n} & 0 & \frac{k-1}{n}
\end{bmatrix} \tag{8}$$

From Eq. (7) the new stiffness matrix for d_k will be

$$S_{d_k}^* = A_k^T S_{d_k} A_k, \tag{9}$$

S_{d_k} being the usual bilinear element stiffness matrix for d_k, dependent of course on n, the interior refinement number. We sum up all of the contributions of the elements

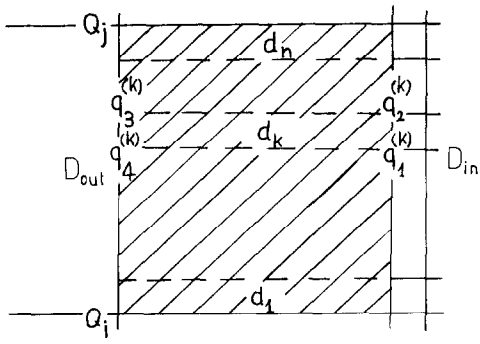

FIG. 3. Typical element d in D_{tr}.

d_k, $k = 1,..., n$, to form the stiffness matrix S_d to be used in the assembly, the unknowns being the terms of the generalized nodal value vector $\mathbf{a}^*$,

$$S_d = \sum_{k=1}^{n} S^*_{d_k}. \tag{10}$$

This element, over which the trial function will be continuous and piecewise bilinear, is a kind of generalization of the 5-node element described by Gregory *et al.* in [2].

The corner elements of D_{tr} are treated likewise. The contribution of these elements is not affected by the size of the mesh in the interior region D_{in}.

By assigning appropriate indices to $a_1,..., a_l$ in the total vector of unknowns, the global stiffness matrix will still have a band structure without a serious increase in the bandwidth, provided that l is not too large, as is indeed the case.

On the other hand, if we consider the regions D_{in} and D_{tr} together as constituting a super-element, we can eliminate $a_1,..., a_l$ by static condensation, leaving only the nodal values in the exterior region as unknowns. In this case, the dimensions of the global stiffness matrix will be affected neither by the number of terms we use in series (1), nor by the number of interior refinements.

Thus, in order to increase accuracy for a given mesh size in the exterior region D_{out}, the mesh in D_{in} can be refined without adding to the number of variables in the final equations.

These refinements in D_{in} should be carried out until the super-element stiffness matrix S_{sup} becomes effectively constant. We then store the final matrix S_{sup}, together with the matrix H_{sup}, which relates the nodal values of the super-element to the values of the coefficients in the series. This relation is given by

$$(a_1,..., a_l)^T = H_{sup}\,\tilde{\mathbf{q}}, \tag{11}$$

$\tilde{\mathbf{q}}$ being the vector of all the nodal values of the super-element.

S_{sup} and H_{sup} having been thus recorded, the super-element can now be included in any finite element mesh in order to solve boundary value problems for various geometries.

3. Test Problem and Numerical Results

In this section we use the method outlined above to compute the displacement field and the stress intensity factor for the case of a two dimensional elastic solid in a rectangle containing an edge crack, subjected to a uniform inplane load T over the ends (Fig. 4).

The material is homogeneous and isotropic with elastic constants $\lambda = \mu = 0.5$. This problem has been solved by Motz in [10] and by Woods in [11] using finite difference methods, and in more recent times by finite element and boundary collocation techniques [2, 3, 12]. The series solution for the displacement in an infinite domain containing a semi-infinite stress-free crack (Fig. 5) takes the form:

$$
\begin{aligned}
2\mu u(r,\theta) = 2\mu u_0 + \sum_{n=1}^{\infty} \{ & \alpha_n r^{n-1/2}[(\eta + n - \tfrac{3}{2})\cos(n-\tfrac{1}{2})\theta \\
& - (n-\tfrac{1}{2})\cos(n-\tfrac{5}{2})\theta] \\
& + \beta_n r^{n-1/2}[-(\eta + n + \tfrac{1}{2})\sin(n-\tfrac{1}{2})\theta + (n-\tfrac{1}{2})\sin(n-\tfrac{5}{2})\theta] \\
& + \gamma_n r^n[(\eta + n + 1)\cos n\theta - n\cos(n-2)\theta] \\
& + \delta_n r^n[-(\eta + n - 1)\sin n\theta + n\sin(n-2)\theta]\},
\end{aligned}
$$

$$
\begin{aligned}
2\mu v(r,\theta) = 2\mu v_0 + \sum_{n=1}^{\infty} \{ & \alpha_n r^{n-1/2}[(\eta - n + \tfrac{1}{2})\sin(n-\tfrac{1}{2})\theta \\
& + (n-\tfrac{1}{2})\sin(n-\tfrac{5}{2})\theta] \\
& + \beta_n r^{n-1/2}[(\eta - n - \tfrac{1}{2})\cos(n-\tfrac{1}{2})\theta + (n-\tfrac{1}{2})\cos(n-\tfrac{5}{2})\theta] \\
& + \gamma_n r^n[(\eta - n - 1)\sin n\theta + n\sin(n-2)\theta] \\
& + \delta_n r^n[(\eta - n + 1)\cos n\theta + n\cos(n-2)\theta]\}, \qquad (12)
\end{aligned}
$$

where $\eta = 3 - 4\sigma$ (plain strain), σ being the Poisson ratio. The polar coordinates are as in Fig. 5, and (u_0, v_0) denotes (u, v) at $r = 0$.

For a finite domain containing a crack, the series (12) can also be used as an approximation to the solution in the neighbourhood of the crack tip.

In view of the symmetry of the domain and the boundary conditions, it is sufficient to solve the problem on the upper half of D, with the appropriate boundary

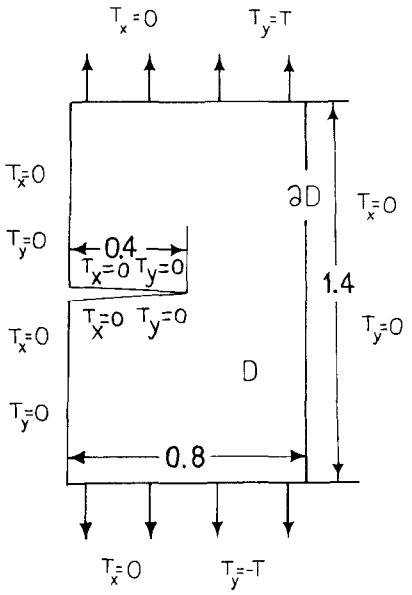

FIG. 4. The model problem.

conditions, as shown in Fig. 6. Because of the symmetry, the coefficients β_n and δ_n in (12) must vanish. Taking $u_0 = v_0 = 0$ and defining

$$a_{2i-1} = \alpha_i, \qquad a_{2i} = \gamma_i, \qquad i \geqslant 1, \tag{13}$$

and $\mathbf{f}_i(r, \theta)$ for $i \geqslant 1$ according to formula (12), we obtain a series of the form (1).

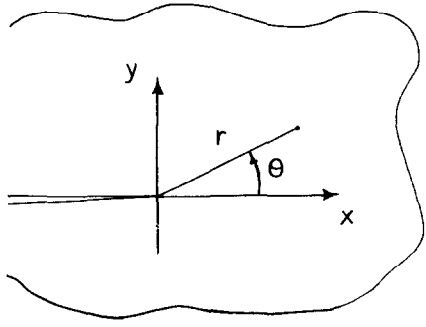

FIG. 5. Crack geometry.

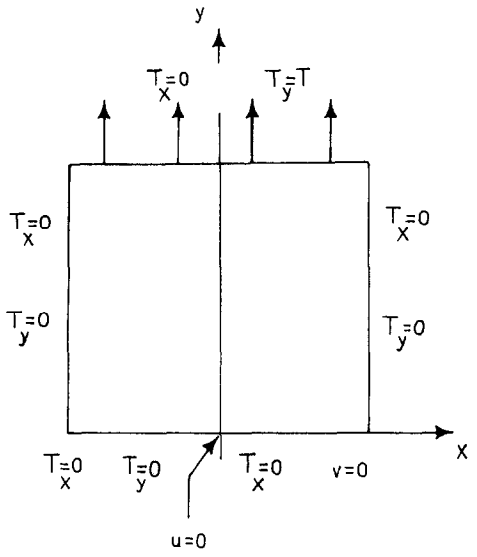

FIG. 6. Domain and boundary conditions as used in the computations.

The calculations were carried out in the displacement formulation in which the potential energy integral to be minimized is [3]:

$$I = \tfrac{1}{2}\iint_D [(\lambda + 2\mu)(u_{,x}^2 + v_{,y}^2) + \mu(u_{,y}^2 + v_{,x}^2 + 2u_{,y}v_{,x}) + 2\lambda u_{,x}v_{,y}]\, dx\, dy - \int_{\partial D_T} (uT_x + vT_y)\, ds. \tag{14}$$

The trial functions for u and v are required to have square integrable first derivatives and to satisfy the essential boundary conditions, which in our case amounts to the vanishing of v for $y = 0$ and $x \geqslant 0$ (Fig. 6). ∂D_T is that part of the boundary on which surface tractions are specified—the entire boundary in the present case. As mentioned in the previous section, bilinear trial functions were used.

The computations were performed using two different exterior meshes, for several internal refinement levels and for a varying number of terms in the series (12). The mesh dimensions in both exterior regions, namely, 0.1×0.0875 (mesh 1) and 0.05×0.04375 (mesh 2), were chosen to make the nodes coincide with those used in Refs. [3, 12]. The dimension of the refinement region $D_{\text{in}} + D_{\text{tr}}$ was 0.4×0.2625, the same for both exterior meshes. Exterior mesh 1 with refinement level $n = 2$ is illustrated in Fig. 7, and exterior mesh 2 with refinement level $n = 4$ in Figs. 8a and b. The applied load was taken to be $T = 0.1$. The values obtained for the displacements are displayed in Tables I–VI.

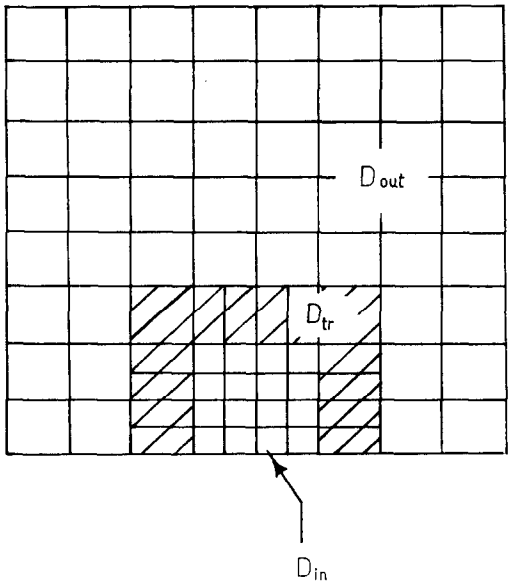

FIG. 7. Exterior mesh 1 (152 degrees of freedom) with interior refinement level $n = 2$.

Table I illustrates the effect of including differing numbers of terms in the series (12) (i.e., of varying l), whilst keeping the number of elements fixed in all three regions. It can be seen that the values converge rapidly with increasing l, and no significant improvement is obtained by including more than eight terms in the series.

The results are, however, further improved by refining the mesh in the interior regions D_{tr} and D_{in}, and the effect of performing this refinement whilst maintaining a fixed mesh in the outer region D_{out} is illustrated in Table II for external mesh 1, and in Table III for external mesh 2.

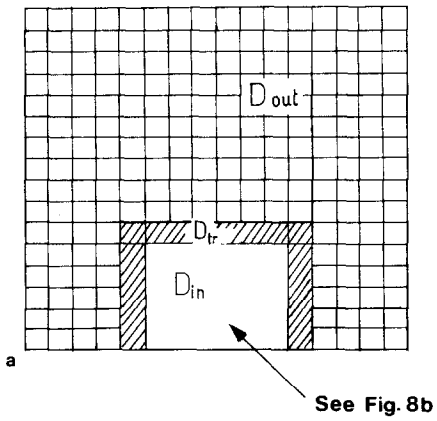

FIG. 8a. Exterior mesh 2 (502 degrees of freedom).

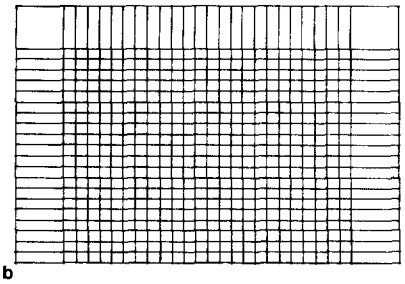

FIG. 8b. Interior region for mesh 2 with interior refinement level $n = 4$.

For a given external mesh size, the difference between the values for successive internal refinements decreases by a factor of approximately one-half, indicating that the values for interior mesh size h differ by a quantity of $O(h)$ from those which would be obtained using an infinite number of internal refinements. We therefore carried out Richardson extrapolation, assuming the error in the displacements to be of the form $\sum_{i=1}^{\infty} c_i h^i$. The results of successive extrapolations at three typical mesh points are listed in Tables IV and V for exterior meshes 1 and 2, respectively. The rapid convergence indicates the correctness of the assumed form for the error. Comparison with the results in Tables II and III shows the extrapolated values to be very close to those obtained with the largest number of internal refinements.

TABLE I

Values of (u, v) for Varying Number of Terms in the Series Using Exterior Mesh 1 for Interior Refinement Level No. $n = 16$

Position			Number of terms l in the series					
x	y		2	4	6	8	10	12
−0.3	0	u	0.046	0.060	0.070	0.069	0.070	0.069
		v	2.089	2.367	2.369	2.369	2.369	2.369
−0.3	0.0875	u	0.421	0.511	0.518	0.519	0.519	0.518
		v	2.093	2.368	2.371	2.371	2.371	2.371
−0.2	0.175	u	0.768	0.954	0.956	0.958	0.958	0.958
		v	1.656	1.849	1.854	1.854	1.854	1.854
0.2	0.175	u	0.591	0.757	0.763	0.764	0.764	0.764
		v	0.173	0.127	0.124	0.124	0.124	0.124
0	0.35	u	1.286	1.576	1.584	1.585	1.585	1.585
		v	0.978	1.014	1.016	1.016	1.016	1.016
0	0.7	u	2.499	2.978	2.991	2.991	2.991	2.991
		v	1.313	1.372	1.374	1.374	1.374	1.374

TABLE II

Values of (u, v) for Varying Interior Refinement Levels
Using Exterior Mesh 1 with Eight Terms in the Series

Position			Internal refinement number n					Extrapolated value
x	y		2	4	8	16	32	
−0.3	0	u	0.045	0.058	0.065	0.069	0.072	0.074
		v	2.141	2.261	2.331	2.369	2.389	2.409
−0.3	0.0875	u	0.461	0.491	0.509	0.519	0.524	0.529
		v	2.143	2.262	2.333	2.371	2.391	2.411
−0.2	0.175	u	0.865	0.913	0.942	0.958	0.966	0.974
		v	1.665	1.765	1.822	1.854	1.870	1.887
0.2	0.175	u	0.675	0.722	0.749	0.764	0.772	0.780
		v	0.115	0.120	1.122	0.124	0.124	0.125
0	0.35	u	1.419	1.506	1.557	1.585	1.599	1.614
		v	0.919	0.970	1.000	1.016	1.025	1.034
0	0.7	u	2.686	2.846	2.940	2.991	3.018	3.045
		v	1.273	1.326	1.357	1.374	1.383	1.392

TABLE III

Values of (u, v) for Varying Interior Refinement Levels
Using Exterior Mesh 2 with Eight Terms in the Series

Position			Internal refinement number n					Extrapolated value
x	y		2	4	8	16	32	
−0.3	0	u	0.063	0.070	0.073	0.075	0.076	0.077
		v	2.295	2.369	2.408	2.429	2.439	2.450
−0.3	0.0875	u	0.502	0.520	0.529	0.534	0.537	0.540
		v	2.297	2.370	2.410	2.430	2.441	2.451
−0.2	0.175	u	0.928	0.958	0.974	0.982	0.986	0.990
		v	1.792	1.853	1.885	1.902	1.911	1.919
0.2	0.175	u	0.742	0.770	0.785	0.793	0.797	0.801
		v	0.122	0.125	0.126	0.127	0.128	0.128
0	0.35	u	1.536	1.589	1.618	1.632	1.640	1.648
		v	0.983	1.014	1.031	1.040	1.044	1.049
0	0.7	u	2.900	2.997	3.050	3.077	3.091	3.095
		v	1.337	1.369	1.387	1.396	1.401	1.405

TABLE IV

Extrapolated Values of (u, v) for Successive Internal Refinement Levels with Eight Terms in Series (12), Using Exterior Mesh 1

Position			Refinement levels used			
x	y		2, 4	2, 4, 8	2, 4, 8, 16	2, 4, 8, 16, 32
−0.3	0	u	0.07053	0.07356	0.07369	0.07369
		v	2.3803	2.4082	2.4092	2.4092
0	0.7	u	3.0060	3.0437	3.0451	3.0451
		v	1.3791	1.3916	1.3920	1.3921
0.2	0.175	u	0.7685	0.7797	0.7801	0.7801
		v	0.1242	0.1251	0.1251	0.1251

The final extrapolated values for exterior meshes 1 and 2 are listed and compared with the results of two other finite element calculations [3] in Table VI. One calculation employed Hermite cubic elements with local mesh refinement (a gradual refinement of the mesh as the singularity is approached) to compute the Airy stress function U at the mesh points. The coefficients in the appropriate series of the form (1) for U were then computed by least square fitting, and the displacements u and v listed in Table VI were obtained by evaluating the corresponding series (12). The other calculations used the stress-hybrid formulation, which yields the displacements at the meshes directly without having recourse to the series expansion. Bilinear stresses were assumed inside the elements and linear displacements along the element boundaries, with local mesh refinement in the neighbourhood of the crack tip.

In both calculations, the elements outside the region of local refinement were of the same size as those in our exterior mesh 1. Our displacements for mesh 1 are seen to

TABLE V

Extrapolated Values of (u, v) for Successive Internal Refinement Levels with Eight Terms in Series (12), Using Exterior Mesh 2

Position			Refinement levels used			
x	y		2, 4	2, 4, 8	2, 4, 8, 16	2, 4, 8, 16, 32
−0.3	0	u	0.07618	0.07678	0.07680	0.07680
		v	2.4423	2.4496	2.4497	2.4497
0	0.7	u	3.0954	3.1051	3.1053	3.1053
		v	1.4020	1.4053	1.4053	1.4053
0.2	0.175	u	0.7980	0.8008	0.8008	0.8008
		v	0.1278	0.1280	0.1280	0.1280

TABLE VI

Extrapolated Values for (u, v) for Meshes 1 and 2 for Eight Terms in the Series, Compared with Those of Ref. [3]

Position			Mesh No. 1	Mesh No. 2	Hermite cubic f.e.m. with local mesh refinement[a]	Stress-hybrid f.e.m. with local mesh refinement[a]
x	y					
−0.3	0	u	0.074	0.077	0.077	0.075
		v	2.409	2.450	2.461	2.415
−0.3	0.0875	u	0.529	0.539	0.542	0.530
		v	2.411	2.451	2.462	2.416
−0.2	0.175	u	0.974	0.990	0.994	0.977
		v	1.887	1.919	1.928	1.893
0.2	0.175	u	0.780	0.801	0.808	0.781
		v	0.125	0.128	0.128	0.125
0	0.35	u	1.614	1.647	1.656	1.619
		v	1.034	1.049	1.053	1.037
0	0.7	u	3.045	3.105	3.063	3.055
		v	1.392	1.405	1.392	1.395

[a] Ref. [3].

TABLE VII

Values of the Coefficients in Series (1) for Varying Interior Refinement Levels Using Exterior Mesh 1 with Eight Terms in the Series

	Interior refinement number					Extrapolated value
	2	4	8	16	32	
$-a_1$	1.055	1.141	1.190	1.216	1.230	1.244
$-a_2$	0.057	0.073	0.084	0.090	0.093	0.096
$-a_3$	0.848	0.869	0.882	0.890	0.894	0.898
$-a_4$	−0.093	0.053	0.115	0.145	0.160	0.174
$-a_5$	−0.236	−0.561	−0.734	−0.824	−0.871	−0.918
$-a_6$	−0.917	−0.578	−0.501	−0.481	−0.474	−0.469
$-a_7$	3.022	1.320	0.812	0.619	0.535	0.460
$-a_8$	1.389	0.449	0.190	0.099	0.061	0.028

TABLE VIII

Values of the Coefficients in the Series for Varying Interior Refinement Levels Using Exterior Mesh 2 with Eight Terms in the Series

	Interior refinement number					Extrapolated value
	2	4	8	16	32	
$-a_1$	1.165	1.211	1.235	1.248	1.254	1.261
$-a_2$	0.077	0.085	0.089	0.091	0.093	0.094
$-a_3$	0.884	0.904	0.915	0.921	0.924	0.927
$-a_4$	0.057	0.087	0.101	0.108	0.112	0.116
$-a_5$	−0.606	−0.713	−0.768	−0.796	−0.811	−0.826
$-a_6$	−0.469	−0.489	−0.505	−0.514	−0.519	−0.524
$-a_7$	1.008	0.951	0.938	0.935	0.935	0.935
$-a_8$	0.230	0.196	0.188	0.186	0.185	0.185

be in excellent agreement with the stress-hybrid values (both calculations use linear trial functions). Our results for mesh 2 are, on the other hand, closer in most cases to the values obtained using Hermite cubic, i.e., higher-order, elements.

The values obtained for the coefficients a_i using the present method are listed in Tables VII and VIII for varying degrees of internal refinement and for the two different exterior meshes, eight terms having been included in the series (12). It can be seen that the convergence with increasing internal refinement is markedly better in the case of the finer external mesh. Again, the deviations from the values which would be obtained using an infinite number of internal refinements are indicated to be of magnitude $O(h)$. The results of the Richardson extrapolation applied to the a_i, $i = 1$–4, assuming the error to be a form similar to that of the displacements, are listed in Table IX for both exterior meshes.

In Table X the final extrapolated values using exterior meshes 1 and 2 are compared with one another, and with the results [3] of two calculations based on the

TABLE IX

Extrapolated Values of $a_1, \ldots, a_4$, for Successive Internal Refinement Levels, for Both Exterior Meshes with Eight Terms in the Series

Refinement levels used	Mesh 1				Mesh 2			
	2, 4	2, 4, 8	2, 4, 8, 16	2, 4, 8, 16, 32	2, 4	2, 4, 8	2, 4, 8, 16	2, 4, 8, 16, 32
$-a_1$	1.2268	1.2430	1.2438	1.2438	1.2565	1.2606	1.2606	1.2606
$-a_2$	0.08999	0.09554	0.09598	0.09599	0.09263	0.09342	0.09368	0.09368
$-a_3$	0.8895	0.8981	0.8985	0.8985	0.9247	0.9272	0.9272	0.9272
$-a_4$	0.1984	0.1708	0.1745	0.1745	0.1164	0.1154	0.1156	0.1156

TABLE X

Extrapolated Values of the Coefficients a_i, $i = 1,\ldots, 8$, for Meshes 1 and 2 Compared with Ref. [3, 12]

	Mesh 1	Mesh 2	Hermite cubic f.e.m. with local refinement[a]	Boundary collocation[b]
$-a_1$	1.244	1.261	1.265	1.265
$-a_2$	0.096	0.094	0.095	0.094
$-a_3$	0.899	0.927	0.935	0.936
$-a_4$	0.175	0.116	0.101	0.100
$-a_5$	−0.92	−0.83	−0.80	−0.80
$-a_6$	−0.47	−0.52	−0.47	−0.46
$-a_7$	0.46	0.93	1.00	1.00
$-a_8$	0.03	0.18	—	—

[a] Ref. [3].
[b] Ref. [12].

Airy stress function formulation. One, as mentioned above, used Hermite cubic finite elements with local mesh refinement, whereas in the second, the a_i were determined by boundary collocation of the series for the Airy stress function using a linear programming technique. Despite the fact that these two techniques are completely different in character, the resulting values of the a_i agree very closely with one another. This indicates that these values are both reliable and accurate and may be used as a benchmark against which the accuracy of other calculations, such as the present one, may be assessed. As is to be expected, mesh 2 gives results somewhat closer on the whole to those obtained by the other methods.

4. Discussion

The results quoted in the previous section show that the method yields accurate results for the displacements and for the coefficients in the series expansion about the singularity. For practical applications such as the determination of the stress intensity factor $-a_1(2\pi)^{1/2}$, a_1 being the first coefficient in the series, only a moderate number of internal mesh refinements are necessary. For example, the results in Table IX show that a_1 for a given exterior mesh may be determined to at least three significant digits by using only refinement levels 2, 4 and 8. For mesh 1 the values obtained differ from the benchmark values by only 1.7% and for mesh 2 the agreement is to within 0.32% (see Table X). On the CDC 6600 computer the total machine time needed for these three refinement levels was 10 sec for mesh 1 and 63 sec for mesh 2. A third of the time is spent on solving the simultaneous linear equations, and most of the remainder is expended on computing the matrices S_e^* from S_e in the interior region D_{in} (see

Eq. (5)). On the other hand, it is not necessary to repeat this part of the calculation for every new case. The interior variables over the refinement region, which are just the coefficients of the series, may be eliminated using static condensation. Thus we obtain a super-element, which may be imbedded in any usual finite element mesh, and in fact the calculations described herein were carried out in this way.

In order to assess the relative merit of the method, it is useful to compare the calculations with those reported in [3]. These latter results were obtained with the aid of *local* mesh refinement, that is, the elements in the neighbourhood of the singularity are taken to be progressively smaller as the singularity is approached, instead of being of uniform size as in the present scheme. The results obtained using the displacement formulation were less accurate than those obtained by the present method. On the other hand, as mentioned above, the stress-hybrid formulation gave displacements which agree closely with the current results for mesh 1. The values of a_1 obtained from the horizontal and vertical displacements lie between the current values for meshes 1 and 2, whilst the rest of the coefficients in the series are less accurate than the current mesh 1 values.

As regards the computing effort required, we note that whereas in the current method the system of equations has to be solved three times for each case (for internal refinement levels 2, 4 and 8), when local mesh refinement is used, the calculation has to be repeated several times for varying degrees of refinement in order to determine when the results have converged. It would, therefore, appear reasonable to adopt the work needed for one solution of the linear equations as a rough measure of the computing effort involved in each scheme. The number of degrees of freedom n is 152 and 502 for meshes 1 and 2, respectively, in the current scheme, compared with 536 for the stress hybrid and 1104 for the Hermite cubic benchmark (both corresponding to the highest degree of local refinement employed). A more acceptable measure of the work involved is the quantity m^2n, where $2m + 1$ is the bandwidth. The values of m^2n are 2.6×10^5 and 3.0×10^6 for meshes 1 and 2 of the current method, respectively, compared with 7.3×10^5 for the stress-hybrid and 1.9×10^7 for the Hermite cubic. These figured indicate that the current method is at least as economical as the stress-hybrid approach with local mesh refinement. In addition, it should be noted that the coefficients of the series are obtained directly, without any resort to further computation. This feature of our method is particularly advantageous when considering configurations involving more than one singular point. In such cases, methods based on determining the a_i from the displacements are liable to yield results which are quite sensitive to the particular fitting procedure chosen. In the present method, on the other hand, each singular point may be surrounded by its own superelement, and the coefficients in the expansion appropriate to each of these points will be determined automatically.

In a further experiment, the stress-hybrid local refinement calculations were modified by constraining the nodal values in the refinement region to agree with the series (12) as in the present method. The resulting improvement was only marginal. We conclude, therefore, that in the region where the nodal values are to be constrained, a uniform refinement should be used, as in the method described herein.

CONCLUSIONS

A modification of the finite element method has been developed for dealing with singular boundary value problems. By taking into account the known form of the solution in the neighbourhood of the singularity, the method enables the mesh to be refined locally without increasing the number of equations to be solved. The coefficients in the series expansion about the singular point are obtained directly from the computation, an important advantage in the application of the method to fracture mechanics for example, where the stress intensity factor is a multiple of the first coefficient. Computations carried out on a test crack problem in linear elasticity gave values for the displacements and the stress intensity factor which were in excellent agreement with the results obtained by other methods. The internal variables over the refinement region may be eliminated using static condensation, thus obtaining a super-element which may be imbedded in the usual finite element mesh. Thus, in fracture mechanics for example, it would be possible to prepare a library of such super-elements of various forms for different material constants, providing a reliable and comparatively cheap tool for the determination of stress intensity factors for various crack configurations.

The method which we have described is quite general, and is capable of application to a variety of singular boundary value problems, provided only that the analytic form of the series solution is known in the neighbourhood of the singularity.

It can thus be used for other cases of singularities arising from the shape of the boundary, for example, the much discussed problem of the eigenvalues of an L-shaped membrane [6]. It is also applicable when the singularity is caused by a discontinuity in the boundary condition, as in the problem in hydrodynamics discussed by Fox and Sankar [13], or when it occurs due to the presence of an interface in the domain, as in the model nuclear reactor problem discussed by Fix *et al.* [6].

ACKNOWLEDGMENTS

We are grateful to Professor J. Aboudi for helpful discussions. The computations were carried out at the Tel-Aviv University Computation Center.

REFERENCES

1. R. WAIT AND A. R. MITCHELL, *J. Comput. Phys.* **8** (1971), 45.
2. J. A. GREGORY, D. FISHELOV, B. SCHIFF, AND J. R. WHITEMAN, *J. Comput. Phys.* **29** (1978), 133.
3. B. SCHIFF, D. FISHELOV, AND J. R. WHITEMAN, *in* "The Mathematics of Finite Elements and Applications," Vol. III (J. R. Whiteman, Ed.), p. 55, Academic Press, New York/London, 1979.
4. J. E. AKIN, *Int. J. Numer. Methods Eng.* **10** (1976), 1249.
5. R. D. HENSHELL AND K. G. SHAW, *Int. J. Numer. Methods Eng.* **9** (1975), 495.
6. G. J. FIX, S. GULATI, AND G. I. WAKOFF, *J. Comput. Phys.* **13** (1973), 209.

7. K. Y. LIN AND J. W. MAR, *Int. J. Fracture* **12** (1976), 521.
8. P. D. HILTON AND G. C. SIH, *in* "Mechanics of Fracture," Vol. I (G. C. Sih, Ed.), p. 426, Noordhoff, Amsterdam, 1973.
9. R. JONES AND R. J. CALLINAN, *Int. J. Fracture* **13** (1977), 51.
10. H. MOTZ, *Quart. Appl. Math.* **91** (1946), 371.
11. L. C. WOODS, *Quart. J. Mech. Appl. Math.* **6** (1953), 163.
12. J. R. WHITEMAN, *in* "Numerical Methods in Fracture Mechanics" (D. R. J. Owen and A. R. Luxmoore, Eds.), p. 128, University of Wales, Swansea, 1975.
13. L. FOX AND R. SANKAR, *J. Inst. Math. Appl.* **5** (1969), 340.